

*Optimization of Backlighter Targets Using a Saturn Ring on the National Ignition Facility*

**Jake Kinney**

Pittsford Sutherland High School

Advisor: Dr. R. S. Craxton

Laboratory for Laser Energetics

University of Rochester

February 2016

## 1. Abstract

Backlighting on the National Ignition Facility (NIF) is a process by which a primary target is irradiated by x rays or protons produced by a secondary “backlighter” target. Uniform spherical implosions of these backlighter targets are ideal to produce high-energy x rays or protons from a small point source at peak compression. In some experiments, the primary target needs to be driven by the NIF beams closest to the equator, leaving only the more polar beams (positioned at  $23.5^\circ$  and  $30.0^\circ$  from the poles) to drive the backlighter target (typically a CH shell with diameter 2 mm and thickness 20  $\mu\text{m}$ ). Given this constraint, it is very difficult to get a uniform implosion even if the beams are repointed to the equator. Using the hydrodynamics simulation code SAGE, a design was developed with a CH “Saturn ring” surrounding the target. The presence of the Saturn ring gave more drive at the target’s equator and allowed for a more uniform spherical implosion. The position of the Saturn ring as well as the beam pointings and defocus were adjusted to produce this optimized design.

## 2. Introduction

Nuclear fusion has the potential to provide the world with abundant clean, safe energy. Fusion relies on fuel found in water rather than oil or gas, and as such does not harm the environment or contribute to global warming. One method to achieve nuclear fusion is to irradiate a spherical target consisting of a glass or plastic shell surrounding cryogenic deuterium and tritium with powerful lasers. When the lasers irradiate the target, the shell ablates outward, causing an opposing force to compress the deuterium and tritium in the interior. The implosion compresses the inner layer to extreme densities. High temperature and pressure in the compressed core provides the kinetic energy needed for the positively charged deuterium and tritium to overcome Coulomb repulsion forces and fuse together.<sup>1</sup> This fusion reaction forms a

helium nucleus and an energetic neutron, which accounts for most of the energy released. The energy in the helium nucleus is redeposited in the fuel in a process known as ignition. Ignition represents the first step towards breakeven, defined as the point at which energy released by fusion is equal to the energy input from the laser. When energy output is substantially higher than energy input, it is known as high gain. High gain is necessary for laser fusion to be used as a plausible energy source.

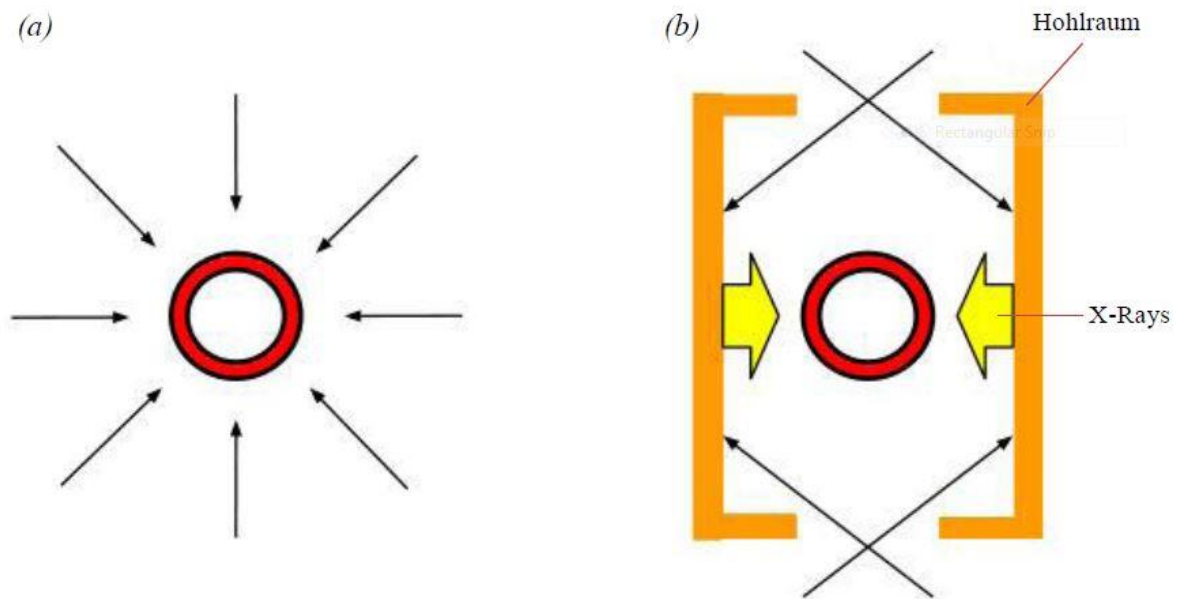


*Figure 1: The two main approaches to laser fusion. (a) Direct drive involves beams striking the target directly. (b) Indirect drive involves beams striking the inner walls of a cylindrical hohlraum, which emits x rays that then irradiate the target. (Figure 1 of Ref. 2).*

Following the description of Ref. 2, there are two main methods of conducting laser fusion, shown in Fig. 1: direct drive<sup>1</sup> and indirect drive.<sup>3</sup> In direct drive, each beam strikes the shell directly, coming in towards the target at normal incidence. The beams are arranged

symmetrically around the shell so that the shell is irradiated from all directions. The OMEGA laser at the University of Rochester's Laboratory for Laser Energetics (LLE) is configured for direct drive. In indirect drive [Fig. 1(b)], laser beams irradiate a cylindrical hohlraum made of a metal with a high atomic number (usually gold) that has been placed around the target. The beams are directed through openings at the top and bottom of the hohlraum to strike the cylinder's inner walls. The hohlraum then re-emits about 80% of the energy it absorbed as x rays, which irradiate the target. There is a significant loss in deposited energy using indirect drive: only 20% of the x rays emitted by the hohlraum are absorbed by the target. A large amount of energy is lost either in the hohlraum walls or through the openings at the ends of the hohlraum. While indirect drive represents an inefficient method of fusion because of the loss in energy, indirect drive does have the advantage of irradiating the target with good uniformity. The National Ignition Facility (NIF)<sup>4</sup> at Lawrence Livermore National Laboratory (LLNL) is configured for indirect drive.

The NIF is currently the most powerful laser in the world; it can deliver a total of 1.8 MJ to a target. It has 192 beams organized in 48 groups of 4 beams each, called "quads" (See Fig. 4 below). The quads are arranged in eight equally spaced rings around the target, with four quads making up each of the two rings closest to the north and south poles and eight quads in each of the two rings above and below the equator. The four rings in both the north and south hemispheres are aligned to strike the target at polar angles ( $\theta$ ) of 23.5°, 30.0°, 44.5°, and 50.0° from the vertical. The locations of the beams in these rings are not conducive to direct drive experiments. If the NIF beams are pointed at the center of the target (as in a direct drive experiment), the resulting implosion does not exhibit good uniformity, as the poles are drastically overdriven in comparison to the equator. In order to execute uniform direct drive

implosions on the NIF, polar drive is used.<sup>5,6</sup> Polar drive is a method in which some of the beams are repointed towards the equator of the target instead of the center of the target. Fig. 2(a) shows an implosion without beam repointing. The poles have been overdriven, resulting in a severely flattened target. As seen in Fig. 2(b), a polar drive implosion involving beam repointing leads to a more uniform spherical implosion. By depositing their energy near the equator, the repointed beams compensate for the lack of quads in the equatorial region.

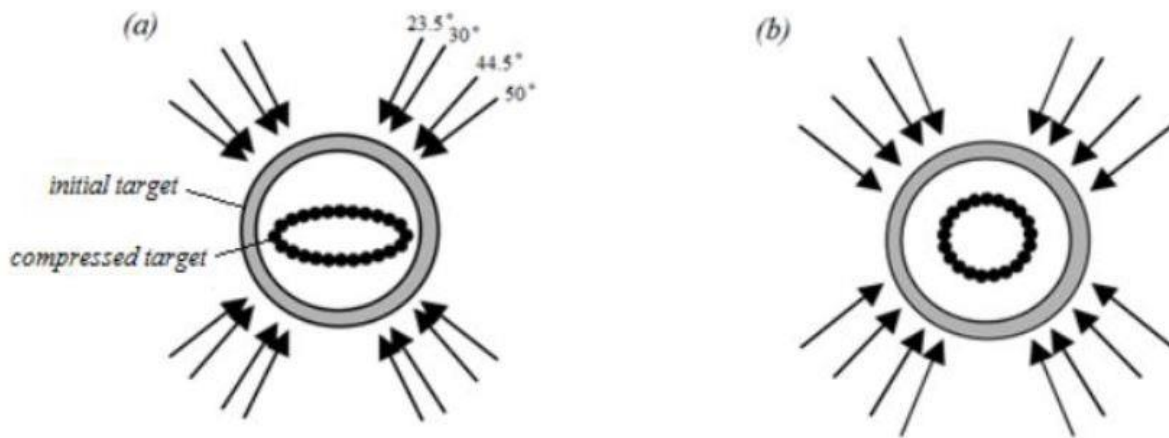


*Figure 2: Polar drive on the NIF. (a) A direct drive implosion on the NIF with the beams pointed at the center results in a nonuniformly compressed target with not enough drive at the equator. (b) Aiming beams towards the equator using polar drive results in a more uniform spherical implosion. (Figure 2 of Ref 2).*

An important use for direct drive implosions is proton or x ray backlighting, first modeled for the NIF in Ref. 2. Backlighting involves using protons or x rays generated by a backlighter target to irradiate a primary target. Due to the presence of multiple targets, two different sets of beams must irradiate each target. Since the majority of NIF beams must be used

to drive the primary target, a limited number of beams can be used to drive the backlighter target. This makes creating a uniform polar drive implosion on a backlighter target extremely difficult. A uniform implosion is desirable because it is ideal to produce a large quantity of protons or x rays emanating from a single point source.

Craxton and Jacobs-Perkins first proposed the addition of a “Saturn ring” around a polar direct drive target on the NIF, to refract beams towards the equator so that more energy will be deposited at the equator.<sup>7</sup> This counteracts the poles being overdriven compared to the equator and leads to a much more uniform spherical implosion. The purpose of this work is to improve the uniformity of backlighter target implosions by adding a Saturn ring around the target. Various parameters have been adjusted in an attempt to create optimized designs. A design has been produced that offers significantly improved spherical uniformity of a backlighter target due to the addition of a Saturn ring.

### 3. Initial Design

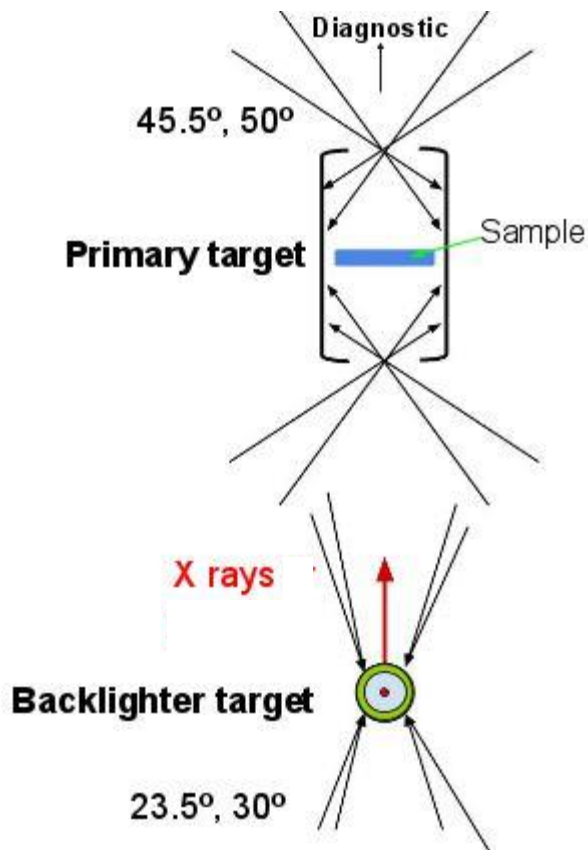
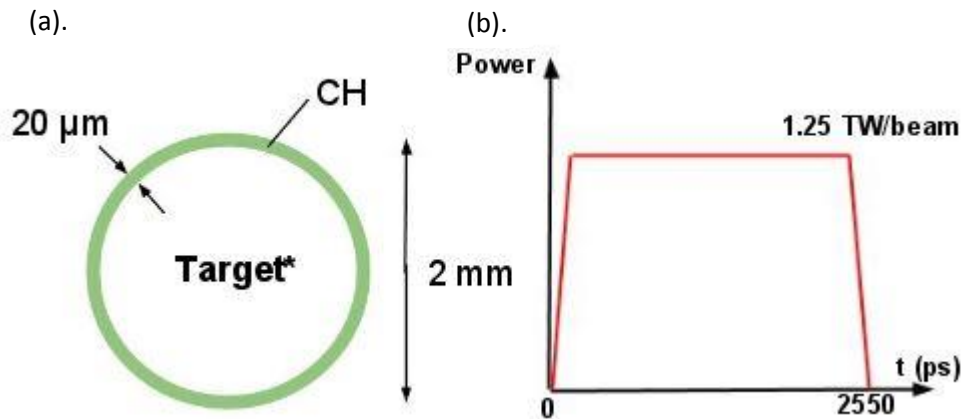


Figure 3: Setup for a backlighter experiment conducted by Heeter et al.<sup>8</sup> The backlighter target is irradiated by rings of beams at 23.5° and 30° from the poles. X rays released from the backlighter implosion pass through the hohlraum, where a primary target is heated by x rays from the hohlraum, to a diagnostic.

At LLNL, Heeter et al.<sup>8</sup> proposed and conducted an experiment on the NIF to test the concept of using a backlighter target to diagnose a primary target. The setup for Heeter's experiment is shown in Fig. 3. The rings of beams at 44.5° and 50.0° from the poles are used for the primary target. This leaves the smaller rings at 23.5° and 30.0° from the poles for the backlighter target. A total of sixteen quads are used for the backlighter, giving 64 beams to drive the target.

As shown in Fig. 4(a), the backlighter target for this NIF experiment consisted of a 20  $\mu\text{m}$  thick CH shell with diameter 2 mm. Each beam carries a 2550 ps pulse with a maximum

power of 1.25 TW/beam [Fig. 4(b)]. These target parameters were used as the starting point for this work. Using the two-dimensional hydrodynamics code SAGE, and the beam parameters from the LLNL design, this experiment was simulated.



*Figure 4: Parameters for the backlighter design used by Heeter et al. (LLNL). (a) The backlighter target is a glass shell,  $20\ \mu\text{m}$  thick and  $2\ \text{mm}$  in diameter. (b) Each beam has a maximum power of  $1.25\ \text{TW}$  with a brief ramp-up time ( $100\ \text{ps}$ ).*

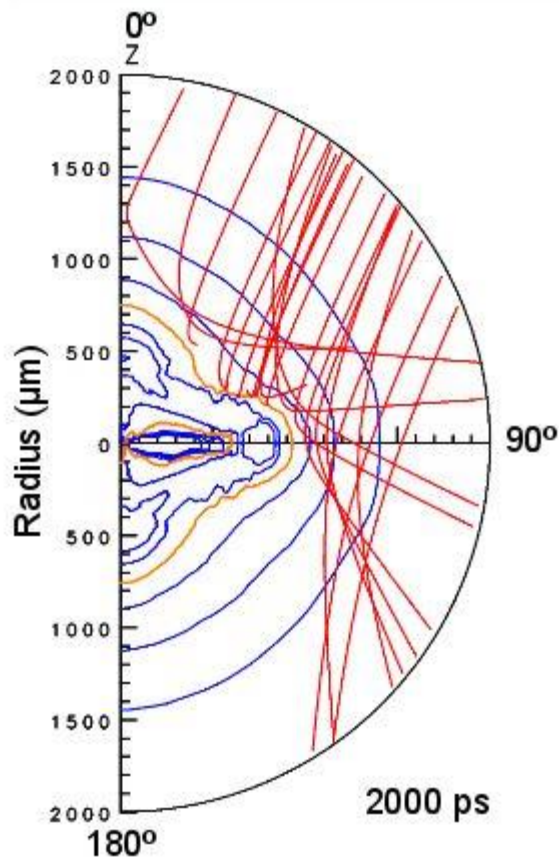


*Figure 5: Raytrace plot showing a simulation of the experiment without a Saturn ring at  $t = 2000$  ps. Red lines indicate the locations of laser rays as they refract through the target. Blue lines are mass density contours of the target. The orange line represents the critical surface beyond which laser rays cannot penetrate. At  $t = 2000$  ps, the equator is severely underdriven and the target is flattened.*

It can be seen clearly in Fig. 5 that the experiment, which did not include a Saturn ring, resulted in poor spherical uniformity. The equator is severely underdriven and the compressed target has simply been flattened. The shape of the orange line, representing the critical surface beyond which laser rays cannot penetrate, can be observed to provide a good approximation to the shape of the shell at a given time. The shell is driven most strongly at around  $45^\circ$  to the  $z$  axis.

Two important ways to measure the effectiveness of the implosion were used. The first measured the radial center of mass as a function of  $\theta$  at different times throughout the implosion. At a given angle  $\theta$  from the pole and a given time  $t$ , the center of mass of the imploding shell will be a certain distance away from the initial center of the target. Center of mass plots such as those

shown in Fig. 6 give these values across an entire hemisphere of the target, from  $\theta = 0^\circ$  (the north pole) to  $\theta = 180^\circ$  (the south pole). In Fig. 6, several of these plots, from different times of a given experiment, are superimposed. These plots provide an easy way to examine the progression of an implosion and see the uniformity. Soon after the start of the implosion, at  $t = 1000$  ps, the areas of the target between the equator and the poles have centers of mass closer to the center of the target than at the poles and especially the equator. At  $t = 2000$  ps, this disparity is much more pronounced. The equator has not been driven enough and the center of mass at the equator remains at over 0.7 mm from the center. At 2000 ps, the root mean square (RMS) deviation on the center of mass plot has a value of 16.1%. This center of mass superposition plot clearly shows the poor uniformity of the original design.

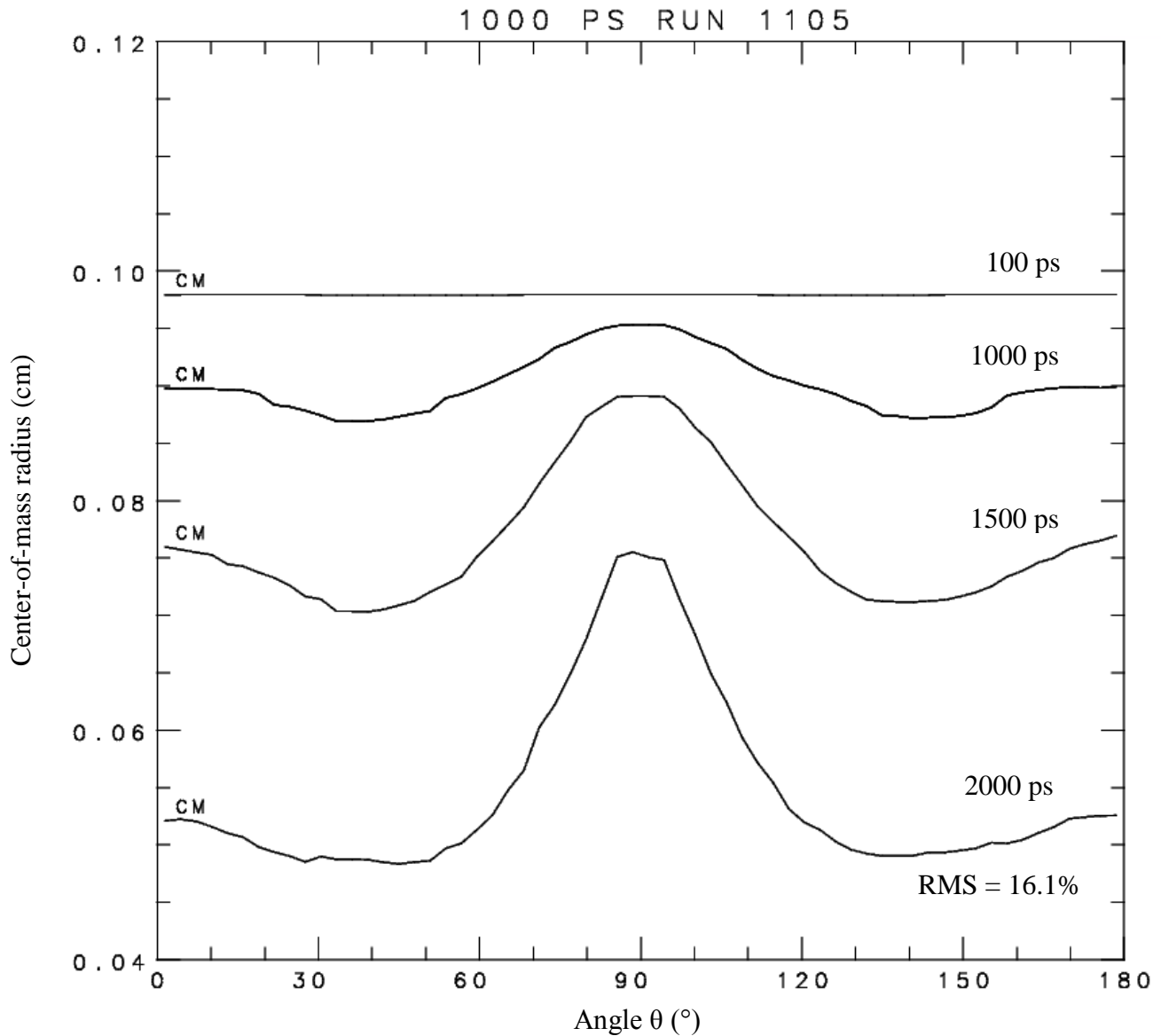
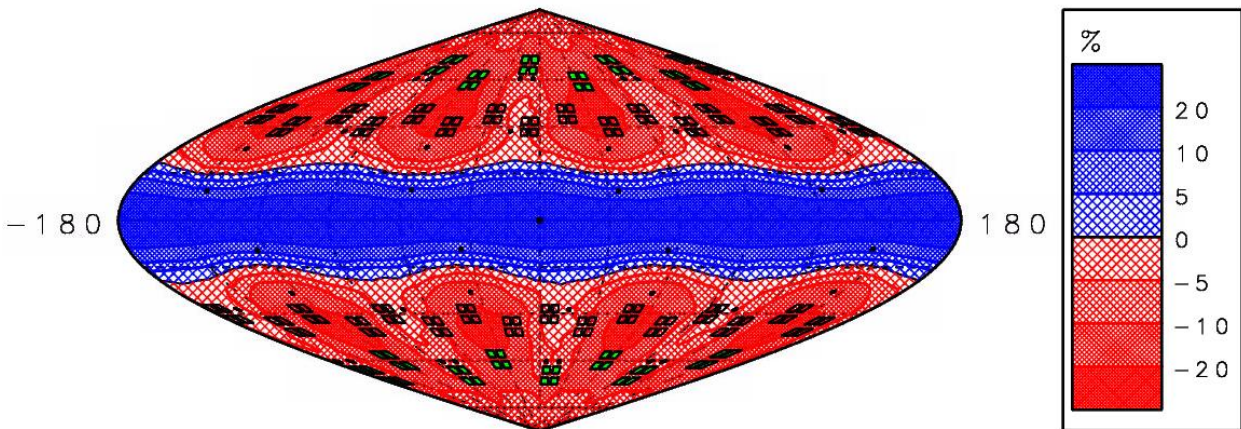


Figure 6: Center of mass radius superposition plot for Heeter’s experiment (without a Saturn ring). As the shell implodes, the equator travels far slower than the poles, leaving the shell severely underdriven around  $\theta = 90^\circ$ .

Another way to study the uniformity of a laser-driven implosion is through a contour plot, such as in Fig. 7, showing the deviation from the average center of mass radius over the whole surface of the target. Fig. 7 is a projection of the entire surface of a sphere. Red areas are

places where the center of mass is closer to the center than average, while blue areas are those where the center of mass is further from the center than average. The outlines of the NIF quads can be seen in black. The black squares shaded with green represent the quads that are used to irradiate the backlighter target. The black dots on the contour plot show where beams have been repointed. The beams were repointed to greater polar angles  $\theta$ , but this was not enough to provide adequate drive to the equator. The contour plot shows very weak drive on the equator, and the strongest drive around  $\theta = 45^\circ$ . This is consistent with Fig. 6. The contour plot shows an RMS of 32.1%. It is worth noting that the contour plots will always have a higher RMS than the center of mass plots, since they take into account differences across the horizontal angle  $\Phi$  rather than just the vertical angle  $\theta$ . These deviation values must be drastically reduced to create an effective backlighter implosion with a small source size and short flash.



*Figure 7: Contour plot of the center of mass radius at 2.0 ns for Heeter's experiment (without a Saturn ring). The blue band surrounding the equator indicates that the region has moved significantly less than average, while the red regions have moved more than average. The z axis is vertical.*

The results of this simulation demonstrated that the implosion on the NIF without a Saturn ring yielded poor spherical uniformity. The beams did not provide adequate drive on the equator and the compressed target was severely flattened instead of imploded spherically.

#### **4. Optimized Design Using a Saturn Ring**

An optimized design was developed in which a Saturn ring was placed around the equator of the target. The purpose of the Saturn ring is to fix one of the major problems with polar drive. Since, by definition, the beams do not strike the target at normal incidence, much of the energy in the beam is not deposited onto the target's surface. This can be seen in Fig. 5, where rays to the right pass through the equatorial region without depositing much energy. However, as shown in Fig. 8, the Saturn ring refracts rays of the beams so that they strike the target with a more desirable angle. As a result, more energy can be deposited at the equator, leading to a more uniform implosion.

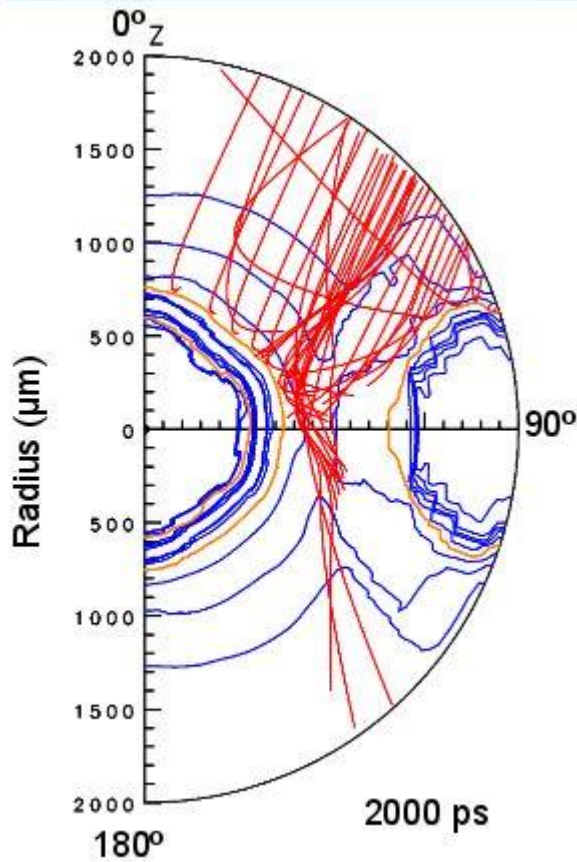


*Figure 8: Raytrace plot showing optimized design with a Saturn ring at  $t = 2000$  ps. Rays (shown in red) refract off the Saturn ring, represented by the blue mass density contours on the right side of the figure. This gives more drive to the equator, resulting in a more uniform spherical implosion.*

Many factors must be taken into account when it comes to optimizing the reaction with the Saturn ring, including shape, size, and position of the ring. The position of the ring is especially important. If the ring is too far away from the target the ring will not refract the beams at all and the beams will interact with the target as if there was no ring. In contrast, if the ring is too close to the target, a phenomenon known as shadowing can occur. The ring will completely obscure the equatorial region from the incoming beams and prevent any of the beams' energy from being deposited on the equator. An intermediate distance must therefore be found that does not lead to either of these problems. Experimentation determined that a radial distance from the surface of the target to the ring of  $400 \mu\text{m}$  was optimal. The shape of the Saturn ring was also varied. The final design took the shape of an irregular pentagon. The flat face on the interior of

the ring, opposite the surface, allows the ring to be placed close enough to the target to effectively refract incoming beams towards the target while not blocking the equatorial region of the target and causing shadowing. It should be noted that the variations explored in the shape of the Saturn ring were by no means comprehensive, and further research should be conducted to further optimize the shape of the ring.

Variations were made in the setup parameters including beam pointing and beam defocus. Each beam in a given quad can be repointed to a different spot on the target's surface through  $\theta$ -shifts and  $\Phi$ -shifts. By repointing beams, the deposited energy can be spread over the entire surface of the target, providing drive everywhere and leading to a uniform implosion. Beam repointings can have a profound impact on the effectiveness of an implosion. For the optimized design, one beam in each of the quads used was pointed to  $\theta = 30^\circ$  from the pole and the remaining three beams in each quad were pointed to  $\theta = 80^\circ$  from the pole.

Because each beam is focused onto the target through a lens, there is a point for every beam that represents the point of best focus. The "defocus" of a beam refers to the distance away from the point of best focus that the target is placed. The larger the defocus of a beam, the larger the area over which its energy is deposited. Defocusing beams has the advantage of depositing energy over a wider area, which is desirable for a uniform spherical implosion; however, there is a tradeoff. Greater defocus means lower overall deposited energy, resulting in a less efficient implosion. The optimum defocus distance was found to be 1.5 cm.

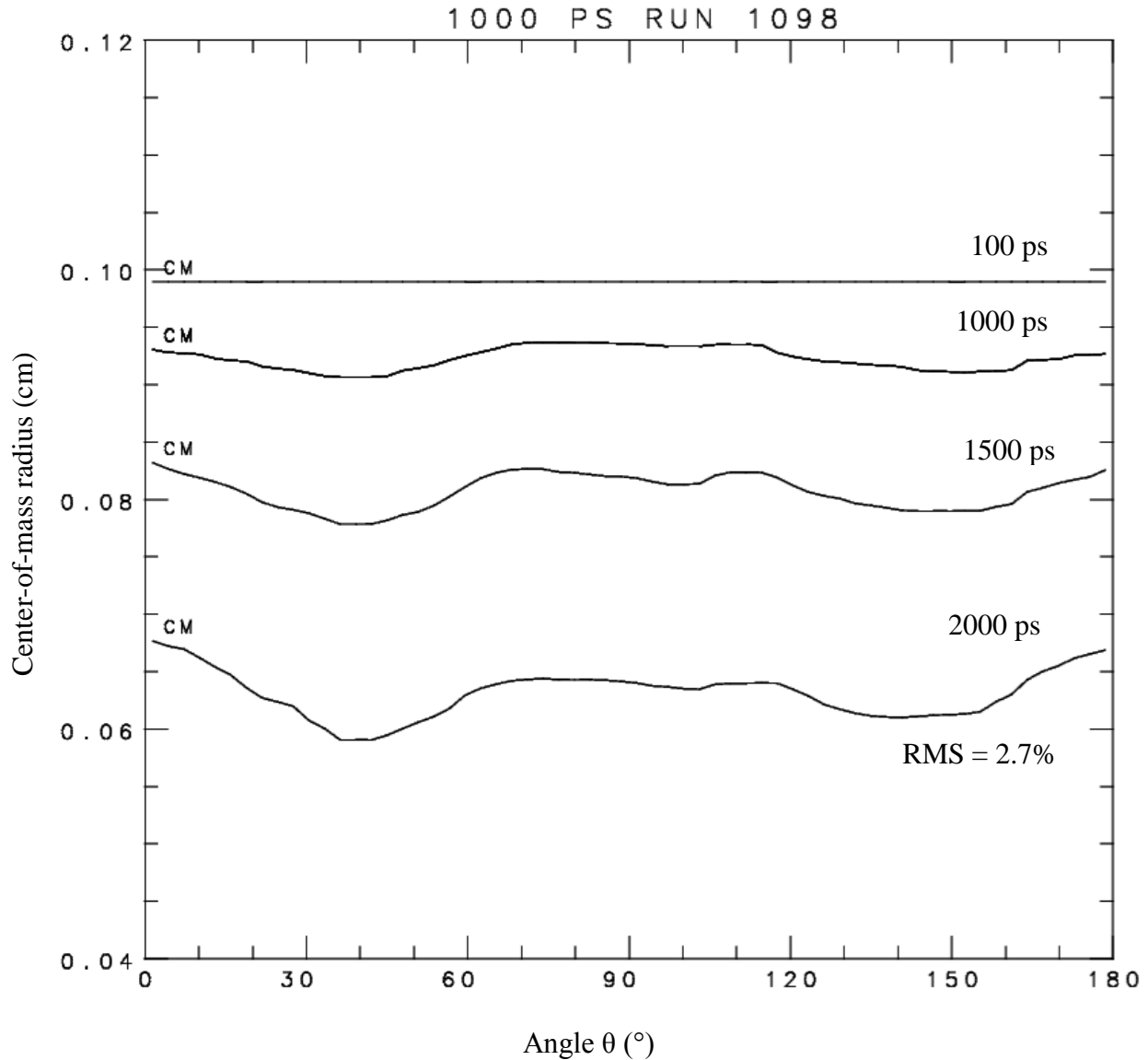
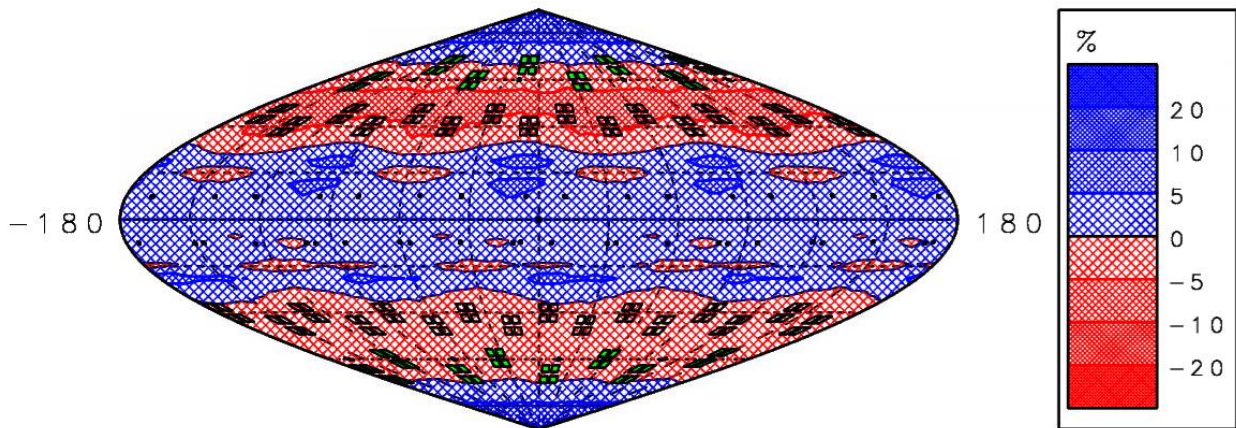


Figure 9: Center of mass radius superposition plot for the optimized design using a Saturn ring. The graph remains much more flat as the surface of the target implodes than in the case without a Saturn ring (Fig. 6). The plot clearly indicates that adding a Saturn ring led to a more uniform implosion.

The optimized design with a Saturn ring produced far greater uniformity than the original design. Center-of-mass radius plots (Fig. 9) for the optimized simulation show an RMS of 2.7%

at 2000 ps, down from 16.1% for the original design. It can be seen in Fig. 9 that the areas at  $45^\circ$  and  $135^\circ$  are still slightly overdriven, and the poles and the equator less so; however, this difference is clearly much more minor than in the original design without the Saturn ring. The flatter center of mass lines in Fig. 9 are indicative of the higher degree of uniformity that results from the addition of the Saturn ring.



*Figure 10: Contour plot of the center of mass radius for the optimized design with a Saturn ring. The lack of darker regions illustrates a more uniform center of mass distribution.*

A contour plot of the center of mass radius for the optimized design, seen in Fig. 10, shows similar improvements, yielding an RMS of 3.4% at 2000 ps, down from 32.1% for the original design. On the optimized design, the poles are slightly above average in terms of center of mass radius, evidenced by the blue color around the poles. The equatorial region is also slightly above average. However, there are few darker regions, indicating that there is less deviation from the average center of mass radius. It can also be seen in Fig. 10 that  $\Phi$ -shifts were added to the beams, demonstrated by the black dots that represent where the beams have been repointed to. These horizontal shifts further improve the uniformity of the implosion. The addition of the Saturn ring gave the equator more drive, producing a near-uniform implosion.

## 5. Scattered Light on the National Ignition Facility

Another advantage provided by adding a Saturn ring to a polar drive backlighter target on the NIF is limiting the amount of scattered light. Scattered light refers to laser rays that do not deposit their energy on the target, but instead go past the target and pass through beam ports on the other side of the target chamber. If these laser rays have enough energy, they can damage the final mirrors in the infrared part of the laser. It is thus desirable to limit the amount of scattered light. It can be seen in the raytrace plot for the experiment without the Saturn ring (Fig. 5) that rays on the edge of the beam pass through low mass densities only, so they do not deposit much of their energy; they are also not refracted very much so they go near the poles. In Fig. 8, the raytrace plot of the Saturn ring experiment, laser rays on the edge of the beam have been blocked and absorbed by the Saturn ring. This reduces the amount of scattered light.

Figures 11 and 12 show contour plots of scattered light for the simulations without the Saturn ring (Fig. 11) and with the Saturn ring (Fig. 12). The red regions represent areas with higher scattered light levels, while the blue regions are areas with less significant scattered light. Regions without significant scattered light have been left unshaded. Fig. 11 shows that scattered light is concentrated at the poles, while the equatorial region does not have much scattered light. With the addition of the Saturn ring, scattered light is still predominantly at the poles, but it is significantly less (as seen in Fig. 12). With the Saturn ring, the equator has no significant scattered light.

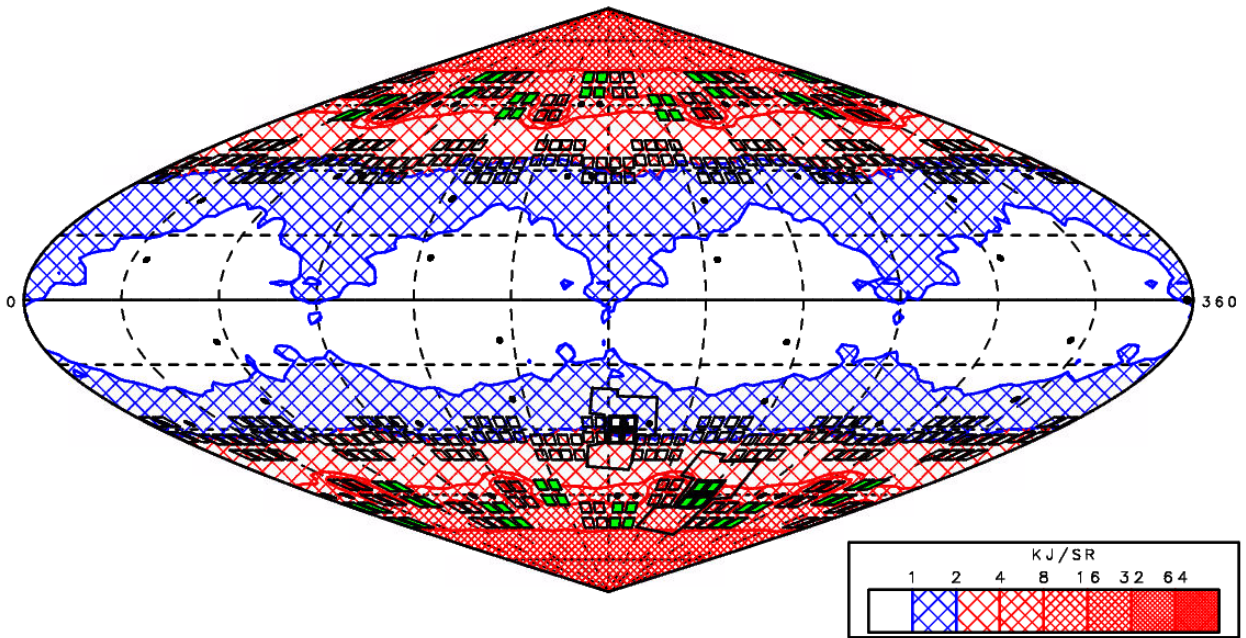
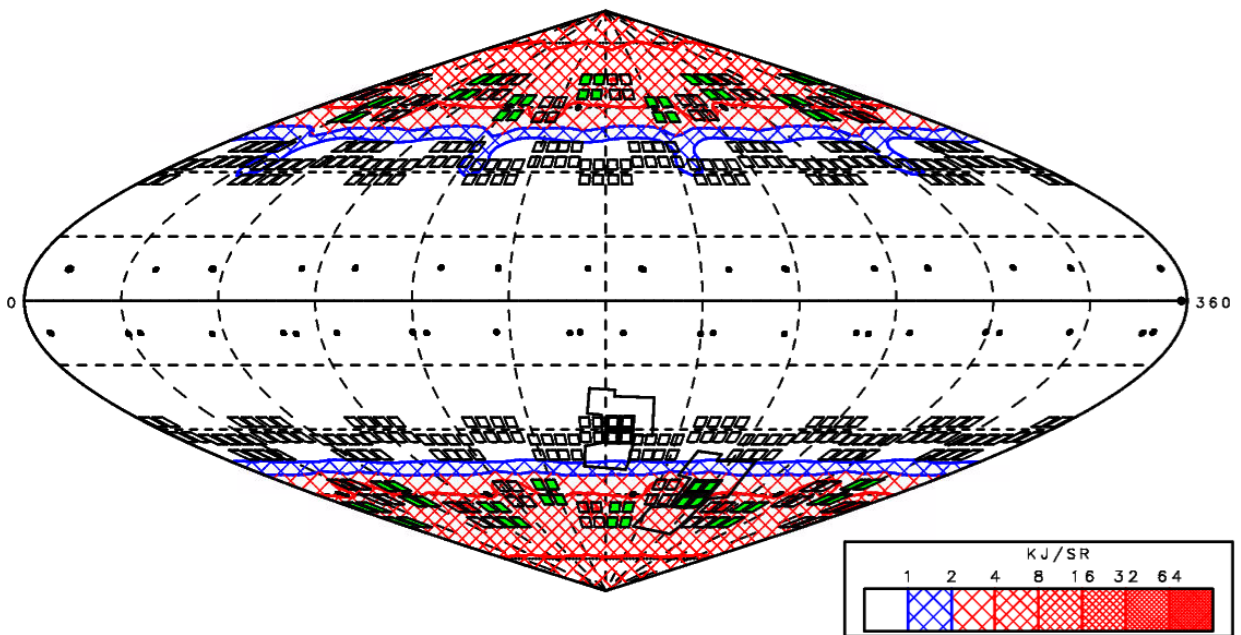


Figure 11: Scattered light on the original design without the Saturn ring. Colored regions indicate levels of scattered light, with red regions representing the highest amount of scattered light detected. The maximum flux is 22.5 kJ/sr.



*Figure 12: Scattered light on the optimized design with a Saturn ring. The level of measured scattered light is drastically reduced, with the maximum flux 9.0 kJ/sr.*

Without the Saturn ring, the highest level of scattered light measured had a peak value of 22.5 kJ/sr. The addition of the Saturn ring lowered this value to 9.0 kJ/sr. The presence of a Saturn ring has clear positive effects on scattered light levels. It should be noted that even the value of 22.5 kJ/sr is considered small and does not pose a problem for experiments with a 2-mm diameter target.

## **6. Simulations of Smaller Targets**

Implosions of smaller targets with diameter 866  $\mu\text{m}$  were also simulated, also irradiated just with beams in the 23.5° and 30° rings. The addition of a Saturn ring produced limited improvement in uniformity. Center of mass radius plots had an RMS of 7.9% at 600 ps in a simulation with a Saturn ring, as compared to an RMS value of 14.7% at 600 ps in a simulation without the ring. While the addition of a Saturn ring did not greatly improve the spherical uniformity of implosions, the presence of the ring drastically reduced the scattered light. The peak scattered light for the simulation with the Saturn ring was 2.8 kJ/sr, while without the ring the peak scattered light had a value of 81 kJ/sr. It is possible that a scattered light level of 81 kJ/sr could have detrimental effects on the laser optics.

## **7. Conclusion**

A design has been developed for a polar drive backlighter target on the National Ignition Facility that uses the addition of a Saturn ring around the target to greatly improve the uniformity of the implosion of the target. The design applies to a specific geometry wherein only rings of beams at 23.5° and 30° from the poles can be used. The presence of the Saturn ring gave lower

RMS deviations of the center of mass radius. A simulation with the Saturn ring produced an RMS value of 3.4%, while the original design without the Saturn ring yielded an RMS value of 32.1%. In addition, the presence of the Saturn ring limited the amount of scattered light produced in the implosion. Designs were also studied for smaller targets, but the addition of a Saturn ring did not greatly improve the uniformity of the implosion. However, the presence of the ring drastically reduced the amount of scattered light on the smaller targets.

## 8. Acknowledgements

I would like to thank Dr. Craxton for his consistent and incredibly helpful advice and feedback throughout this process, as well as for running the High School Program. I would like to thank the Laboratory for Laser Energetics for the wonderful opportunity to take part in the High School Program; it has been a rewarding and informative experience in scientific research.

## References

- 
1. J. Nuckolls et al., "*Laser Compression of Matter to Super-High Densities: Thermonuclear (CTR) Applications*," *Nature* 239, 139 (1972).
  2. Yifan Kong, "*Beam-Pointing Optimization for Proton Backlighting on the NIF*," Laboratory for Laser Energetics High School Summer Research Program (2013).
  3. J. Lindl, "*Development of the Indirect-Drive Approach to Inertial Confinement Fusion and the Target Physics Basis for Ignition and Gain*," *Phys. Plasmas* 2, 11 (1995).
  4. C. A. Haynam et al., "*National Ignition Facility Laser Performance Status*," *Applied Optics* 46, 16 (2007).
  5. S. Skupsky et al., "*Polar Direct Drive on the National Ignition Facility*," *Phys. Plasmas* 11, 5 (2004).

6. R. S. Craxton et al., “*Polar Direct Drive: Proof-of-principle Experiments on OMEGA and Prospects for Ignition on the National Ignition Facility*,” Phys. Plasmas 12, 056304 (2005).
7. R. S. Craxton and D. W. Jacobs-Perkins, “*The Saturn Target for Polar Direct Drive on the National Ignition Facility*,” Phys Rev. Lett. 94, 095002 (2005).
8. R. F. Heeter, Lawrence Livermore National Laboratory, private communication.